CIRP Annals - Manufacturing Technology 70 (2021) 309–312

Contents lists available at ScienceDirect

CIRP Annals - Manufacturing Technology

journal homepage: https://www.editorialmanager.com/CIRP/default.aspx

Active control of high frequency chatter with machine tool feed drives in turning

Alper Dumanli, Burak Sencer*

Oregon State University, Corvallis, USA

Submitted by László Monostori, Budapest, Hungary

ARTICLE INFO

Article history:
Available online 20 May 2021

Keywords:
Chatter
Vibration
Control

ABSTRACT

This paper presents a new active vibration control strategy to mitigate high frequency regenerative chatter vibrations using machine tool feed drives. Rather than modal damping, proposed approach aims to control regenerative process dynamics to shape the Stability Lobe diagram (SLD) and attain higher material removal rates. The controller is designed as a feedback filter whose parameters are optimized to compensate regeneration. The proposed strategy is applied to actively control orthogonal (plunge) turning dynamics where >2.5 [kHz] chatter vibrations are suppressed by a fast tool servo (FTS) drive system. Stability lobes are shaped locally to reach up to 4x higher material removal rates.

1. Introduction

Chatter vibrations have been a limiting factor for attaining larger material removal rates (MRR) in turning for decades [1]. They originate due the flexibilities (resonances) in the workpiece-machine-tooling structure and by the regeneration effects [1,2]. Overall process-machine interaction can be modelled by a delay differential equation (DDE), and chatter-free cutting conditions are selected from Stability Lobe Diagrams (SLDs). Nevertheless, practical spindle speeds in turning are lower and when structural resonances are at high frequency, conventional SLDs have densely packed narrow lobes that cannot be used to maximize MRRs [2].

The overreaching goal has been to exceed stability limitations in turning, and it can be attained by shaping SLDs in two major ways; firstly, regeneration effect is targeted through process parameter selection such as exploiting process damping [3], optimizing tool geometry/posture [4], or by spindle speed variation (SSV) [2]. These efforts shape SLDs locally to create stable pockets to reach higher MRRs and are designed to work on a pre-determined spindle speed region.

Another approach focuses on damping structural resonances by passive or active systems [2,5–10]. Increasing modal damping lifts SLDs up, which delivers moderate stability increase over a wider spindle speed range. Tuned-mass-dampers (TMD), or tools with friction dampers [2] are widely used in practice, and their robustness can be enhanced semi-actively [8,9]. However, fully active systems are much more effective since they can dampen multiple modes [7], integrate within machine elements [9], and even be realized by using machine's existing feed drives [10]. A fundamental requirement for effective active damping is that targeted resonances must lie within the control bandwidth of the actuator or feed drive system, which limits their practical usage to dampen modes within ~200 Hz range [2,10]. Control algorithms based on direct velocity [6,8] or acceleration feedback [10] are widely used. However, when low frequency resonances are damped actively, the lightly damped high frequency modes become destabilized. Therefore, loop shaping based tuning should be practiced [10], or model-based techniques such as H∞, μ-synthesis or delayed feedback [7,11,12] can be employed. Still, fundamental limitation of modal damping-based chatter control techniques is that they rely on servo control or inertial actuator bandwidth, which cannot be widened enough to dampen high frequency modes.

This paper presents a novel active chatter vibration control strategy for machine tool feed drives. As opposed to injecting modal damping by servo loop shaping [5–10], proposed controller is designed to achieve process loop shaping, which focuses on controlling regenerative machining process dynamics using machine tool feed drives. This approach brings two major advantages over state of the art. Firstly, core cause of chatter; regeneration effects are suppressed, which allows local shaping of SLDs to significantly increase MRR. Secondly, it allows control of high frequency chatter that is beyond the closed-loop positioning bandwidth of feed drives. Fig. 1a depicts the proposed scheme. Proposed controller is designed as an add-on compensator (filter) strapped around the existing position controller to suppress chatter vibrations. Thus, both low frequency position control and high frequency chatter mitigation are achieved jointly. Following sections explain design, tuning and experimental validation of proposed approach in orthogonal (plunge) turning using a fast tool servo (FTS) drive system.

2. Loop transmission dynamics of orthogonal cutting

Fig. 1 illustrates the well-known dynamics of orthogonal turning [1,2] with a flexible tool assembly carried by a feed drive system. Dynamic chip thickness $h(s)=L\{h(t)\}$ and feed forces $f(s)$ generated by current vibration of the tool tip $y(s)$ and the one left on part surface in previous spindle revolution, $e^{-sT}y(s)$:

$$h(s) = h_0 - \left[y(s) - e^{-sT}y(s)\right], f(s) = K_F a h(s) \quad (1)$$

where s is the Laplace operator, T is the spindle (delay) period, h_0 is intended (static) chip thickness, K_F is the cutting force coefficient,

* Corresponding author.
E-mail address: burak.sencer@oregonstate.edu (B. Sencer).

https://doi.org/10.1016/j.cirp.2021.04.060
0007-8506/

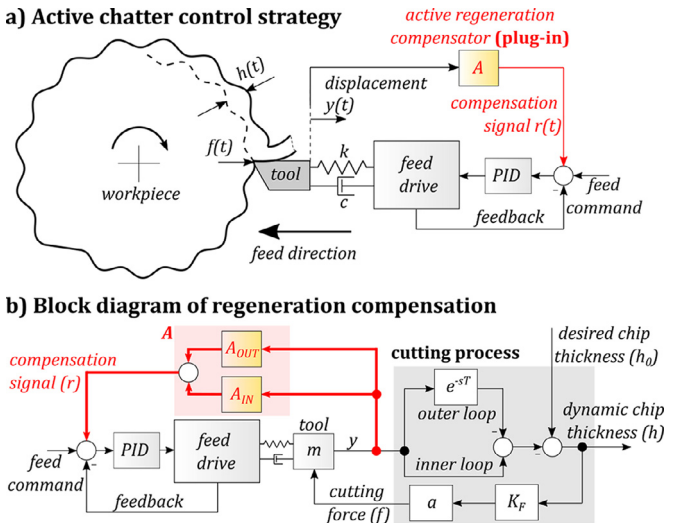

Fig. 1. Illustration (a) and block diagram (b) of the proposed strategy.

and a is width (depth) of cut. Cutting forces excite the flexible structure and produce current vibrations as:

$$y(s) = G(s)f(s) = G(s)K_F a\left(h_0 - \left[y(s) - e^{-sT}y(s)\right]\right) \tag{2}$$

where $G(s)$ is the transfer function of the flexible tooling system. Laplace operator (s) is dropped from signals and functions in the remainder, and Eq. (2) is expressed in transfer function form as:

$$\frac{y}{h_0} = \frac{K_F aG}{1 + aK_F G(1 - e^{-sT})} = \frac{K_F aG}{1 + aL_P} \tag{3}$$

where the L_P=$K_F G(1\text{-}e^{-sT})$ term in Eq. (3) is the so-called "process loop transmission" dynamics with a being the process gain. Fig. 2 shows its characteristics for a delay period, T. Process loop transmission follows amplified flexible tooling dynamics $K_F G$ but modulated by the delay term ($1\text{-}e^{-sT}$), which contains the "regenerative effects" and introduces gain and phase ripples. It is due to those ripples that phase of L_P drops below −180[deg] right after the resonance (ω_n), which marks the "chatter frequency" (ω_c) and determines min. gain margin of the process (See Fig. 2b). Note that limit width of cut becomes a_{lim}=1/|$L_P(j\omega_c)$|. SLDs are generated scanning gain margin of L_P over a set of spindle speeds.

The following sections present the design of the vibration compensator that actively uses machine tool feed drives to shape the process loop transmission of Eq. (3).

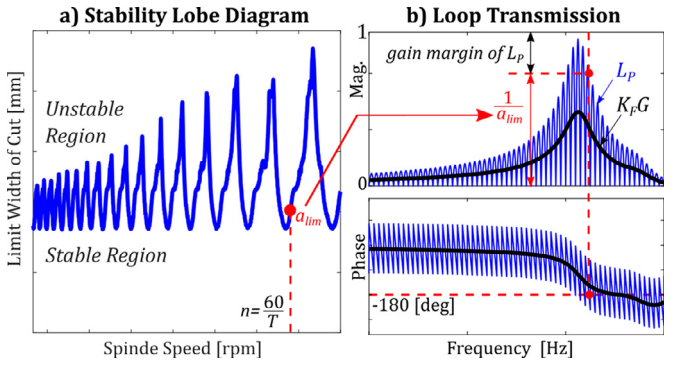

Fig. 2. SLDs and Process Loop Transmission Dynamics.

3. Design of active regeneration cancelling compensator

Block diagram of proposed control scheme is given in Fig. 1b. As shown, an add-on compensator (filter) is designed that injects a position compensation signal r based on the tool vibration measurement y. Its design is based on cancelling the inner and outer regeneration effects to shape the SLDs and to maximize the limit width of cut a_{lim} around a desired spindle (cutting) speed region. Therefore, it is called the Active Regeneration Compensator (ARC) and denoted by the transfer function, A.

With the introduction of ARC signal r, the augmented tool tip and process dynamics can be derived from Eq. (2) and Fig. 1b as:

$$y = Gf + AT_T y \rightarrow y = K_F aG\left[h_0 - y(1 - e^{-sT})\right] + AT_T y \tag{4}$$

where T_T=y/r is the tool tip tracking transfer function of feed drive system, which is typically governed by a low-bandwidth industrial PID controller. Eq. (4) can be put in a transfer function form as:

$$\frac{y}{h_0} = \frac{K_F aG}{1 + K_F aG(1 - e^{-sT}) - AT_T} = \frac{K_F aG}{1 + L_{ARC}} \tag{5}$$

which reveals that the modified process loop transmission L_{ARC}=$K_F aG$ ($1\text{-}e^{-sT}$)-AT_T is augmented by the ARC filter, A.

In order to effectively alter stability margins of L_{ARC}, A is designed with two parts: A=A_{IN}+A_{OUT}. A_{IN} targets the inner modulation loop to suppress effect of current tool vibration y, whereas A_{OUT} targets the delayed feedback dynamics due to the outer regeneration loop, $e^{-sT}y$. Eq. (5) can be re-written explicitly in terms of those A_{IN} and A_{OUT} components as:

$$\frac{y}{h_0} = \frac{K_F aG}{1 + \underbrace{(K_F aG - A_{IN}T_T)}_{\substack{\text{inner modulation}\\ \text{cancellation}}} - \underbrace{(K_F aGe^{-sT} + A_{OUT}T_T)}_{\substack{\text{outer modulation}\\ \text{cancellation}}}} \tag{6}$$

Following sections present design of A_{IN} and A_{OUT} compensators to cancel the inner and outer modulation effects shown in Eq. (6).

3.1. Design of the outer modulation compensator (A_{OUT})

A_{OUT} is designed to suppress the effect of outer modulation. Notice from Eq. (6) that if A_{OUT} could be ideally chosen as:

$$A_{OUT} = -K_F aGT_T^{-1}e^{-sT} \tag{7}$$

effect of outer regeneration is completely cancelled. a is the desired stable depth of cut, and G is the disturbance response of tool/feed drive system, which can be measured by tap-testing. However, the inverse of higher-order closed-loop tracking dynamics, T_T^{-1} term, cannot be realized on a practical system due to servo phase losses and non-minimum phase zeros [6,10]. Therefore, its delayed realization, the $T_T^{-1}e^{-sT}$ term in Eq. (7) is considered. The idea is to approximate -$T_T^{-1}e^{-sT}$ by an N^{th} order FIR filter within a meaningful frequency band $\omega \in [\omega_1, \omega_M]$ as:

$$P_{OUT} = p_1 z^{-T_1/T_s} + p_2 z^{-T_2/T_s} + \cdots + p_N z^{-T_N/T_s} \approx -T_T^{-1}e^{-sT}, \quad z = e^{sT_s} \tag{8}$$

with T_s being position loop sampling time. Frequency band [ω_1,ω_M] is selected to confine chatter frequency by setting ω_1=ω_n and ω_M is set reasonably larger. Notice that the delay T is known at a given spindle (cutting) speed, T = 60/n. Filter delays $T_1 \ldots T_N$ are selected centred around that spindle period [$T_1 \ldots T_N$]↔[T-2π/$\omega_1 \ldots T$+ 2π/ω_1] to ensure causal inversion of T_T. Finally, gains of the FIR filter $p_1 \ldots p_N$ are determined to minimize its fitting discrepancy from system inverse, min||P_{OUT}+$T_T^{-1}e^{-sT}$|| by:

$$\min_{p_1 \cdots p_N} \left(\begin{array}{l} \text{Re}\{P_{OUT}(j\omega)T_T(j\omega) + e^{-j\omega T}\}^2 \\ + \text{Im}\{P_{OUT}(j\omega)T_T(j\omega) + e^{-j\omega T}\}^2 \end{array} \right) \text{ forall } \omega \in [\omega_1, \quad \omega_M] \tag{9}$$

which can be put in a matrix-vector form as:

$$\min_{\mathbf{p}=p_1 \cdots p_N} \| \Lambda \mathbf{p} + \boldsymbol{\nu} \|_2^2, \quad \text{where}:$$

$$\Lambda = \begin{bmatrix} \text{Re}\{e^{-j\omega_1 T_1}T_T(j\omega_1)\} & \cdots & \text{Re}\{e^{-j\omega_1 T_N}T_T(j\omega_1)\} \\ \vdots & \ddots & \vdots \\ \text{Re}\{e^{-j\omega_1 T_1}T_T(j\omega_M)\} & \cdots & \text{Re}\{e^{-j\omega_1 T_N}T_T(j\omega_M)\} \\ \text{Im}\{e^{-j\omega_1 T_1}T_T(j\omega_1)\} & \cdots & \text{Im}\{e^{-j\omega_1 T_N}T_T(j\omega_1)\} \\ \vdots & \ddots & \vdots \\ \text{Im}\{e^{-j\omega_1 T_1}T_T(j\omega_M)\} & \cdots & \text{Im}\{e^{-j\omega_1 T_N}T_T(j\omega_M)\} \end{bmatrix} \tag{10}$$

$$\boldsymbol{\nu} = [\ \cos(\omega_1) \quad \cdots \quad \cos(\omega_M) \quad \sin(\omega_1) \quad \cdots \quad \sin(\omega_M)\ ]^T$$

where M is the frequency resolution. Eq. (10) is a convex optimization (least squares fitting) problem, which can be solved efficiently to determine FIR gains, and A_{OUT} is implemented as:

$$A_{OUT} = K_F a G P_{OUT} \tag{11}$$

An illustrative example is provided in Fig. 3. When A_{OUT} is implemented, delay-induced phase ripples are robustly attenuated within $[\omega_1, \omega_M]$. As a result, 180 [deg] phase crossing is shifted to high frequency, which increases gain margin of process loop transmission providing larger stable depth of cut (a_{lim}).

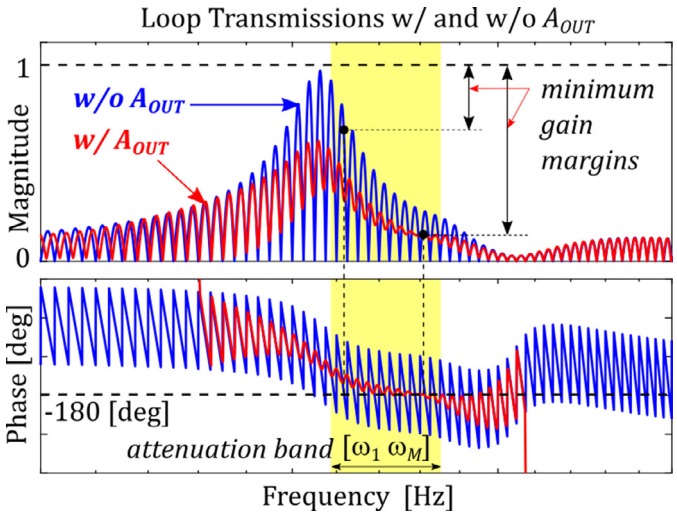

Fig. 3. Outer regeneration cancellation using A_{OUT}.

3.2. Design of the Inner Modulation Compensator (A_{IN})

The A_{IN} compensator is designed to further increase a_{lim} around a targeted spindle speed by cancelling the effect of inner modulation. To cancel the inner modulation terms (see Eq. (6)), A_{IN} is selected in the form of:

$$A_{IN} = -K_F a G \hat{T}_T - 1 P_{IN} \tag{12}$$

where $\hat{T}_T - 1$ is an approximate, causal inverse of feed drive's tracking dynamics, which neglects non-minimum phase zeros. Design of the P_{IN} filter in Eq. (12) is critical. Similar to the design of A_{OUT} compensator, P_{IN} is selected as simple K^{th} order FIR filter:

$$P_{IN} = q_0 + q_1 z^{-1} + \cdots + q_K z^{-K}, \quad z = e^{sT_s} \tag{13}$$

whose parameters $q_0 \ldots q_K$ are determined to maximize a_{lim} by minimizing the real part of process loop transmission. Based on Eq. (6), this parameter search is set as an optimization problem:

$$\min_{q_0 \cdots q_K} \left(\frac{1}{a_{\lim}} \right) \text{subject to :}$$
$$-\mathrm{Re}\left\{ \underbrace{\left(K_F G - \underbrace{K_F G T_T \hat{T}_T^{-1} P_{IN}}_{A_{IN} T_T / a} \right)}_{\text{Inner modulation}} \underbrace{- \left(K_F G e^{-sT} + T_T A_{OUT}/a \right)}_{\text{Outer modulation}} \right\} \le \frac{1}{a_{\lim}} \tag{14}$$

Above optimization problem has two key elements. Firstly, the objective function tries to minimize $1/a_{lim}$, whereas its only constraint tries to keep the negative real part of loop transmission below that. Therefore, optimal filter parameters are sought that maximizes gain margin of the process by pushing the real crossing of process loop transmission to right-hand side of the complex plane. This parameter search is governed by Eq. (14), and it is in fact a convex optimization problem that can be solved conveniently using linear programming to determine the best filter parameters. With the P_{IN} filter determined from Eq. (14) proposed ARC design, $A = A_{OUT} + A_{IN}$ is implemented from Eqs. (11) and (12) as shown in Fig. 1b.

4. Experimental validation

The experimental turning system setup used in validating proposed active chatter avoidance strategy is shown in Fig. 4. Orthogonal tube cutting experiments are conducted on a Al6061 workpiece with a carbide insert, yielding roughly K_F=~1338 [N/mm^2]. A Dytran 3035B1G accelerometer with 10 [mV/g] sensitivity is used to measure the tooling dynamics G, and Fig. 4b shows measured and fitted FRFs. Notice that due to slender tool shank the system suffers from a dominant mode at ~2.57 [kHz].

As shown, the tool (shank) is fed to the workpiece by a piezo actuated FTS feed drive system. Details of the FTS system can be found in [13]. The actuator assembly contains an internal displacement sensor, which allows tuning a dedicated collocated PID controller with a maximum tracking bandwidth of 1 [kHz] shown in Fig. 4c (see blue line, x/r). The sampling frequency of the real-time control system is set to 50 [kHz]. Tool tip tracking transfer function ($T_T = y/r$) is measured by integrating the tool tip acceleration measurements and shown in Fig. 4c.

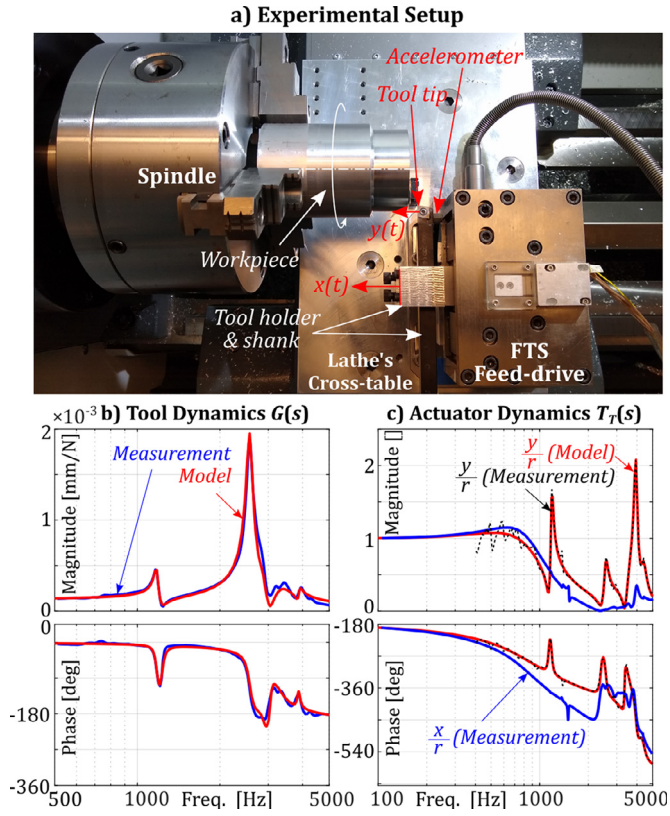

Fig. 4. Experimental setup and its dynamic characterization.

Proposed active control algorithm ARC is first designed to suppress chatter due to the dominant mode at ~2.57 [kHz] (See Fig. 4b) by selecting the target frequency band as $\omega \in [2500, 2800]$ [Hz]. The objective is to open up a stable pocket at around $n = 1800$ [rpm]. FIR filter orders of A_{IN} and A_{OUT} are set as $N = 20$, $K = 5$. Note that in realization of ARC, tool tip vibrations (y) are estimated from integrating accelerometer measurements and high-pass filtering with 250[Hz] cut-off.

Fig. 5 shows the original and shaped process dynamics by ARC. As shown in Fig. 5a, A_{OUT} eliminates ripples due to the regeneration effect, and A_{IN} further minimizes the negative real part of process loop transmission. This improves the gain margin of the process significantly. It is also evident from Fig. 5b that process loop transmission is squeezed and pushed to the right-hand side of complex plane and the -1 point by the help of ARC.

Next, SLDs are plotted in Fig. 6a. As shown, due to high frequency resonance (~2.57 [kHz]), the original stability lobes are very tight, and asymptotic stability limit is below ~0.5 [mm]. However, when ARC is used, stability is drastically improved around the desired 1800 [rpm]. Widths of cut up to ~2 [mm] can be cut stably providing 4 × improvement in productivity. Tube cutting experiments (plunge turning) at a feedrate of 4[μm/rev] are conducted. As shown, workpieces with 0.5–1.75 [mm] wall thicknesses are machined free of chatter with a smooth surface finish by the help of the proposed ARC design.

Fig. 6b shows the effect of ARC when it is switched on during machining at 1.75 [mm] width. When ARC is turned on at ~2.5 [s], chatter vibrations at 2.66[kHz] are quickly dampened, and the

process is stabilized. ARC suppresses chatter vibrations originating from a mode beyond positioning bandwidth (~1 [kHz]) of the feed drive. This provides flexibility since servo controller can be designed separately for positioning, and ARC is activated to suppress chatter when needed. To suppress high frequency chatter with ARC, drives must be able to respond to small (micron level) position commands at that high frequency. In practice this requires their open loop response to be measurable, and not limited by their power rating.

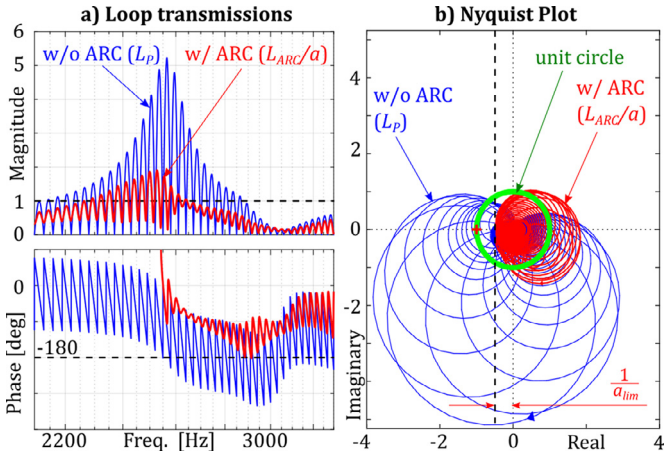

Fig. 5. Process loop transmissions with and without ARC.

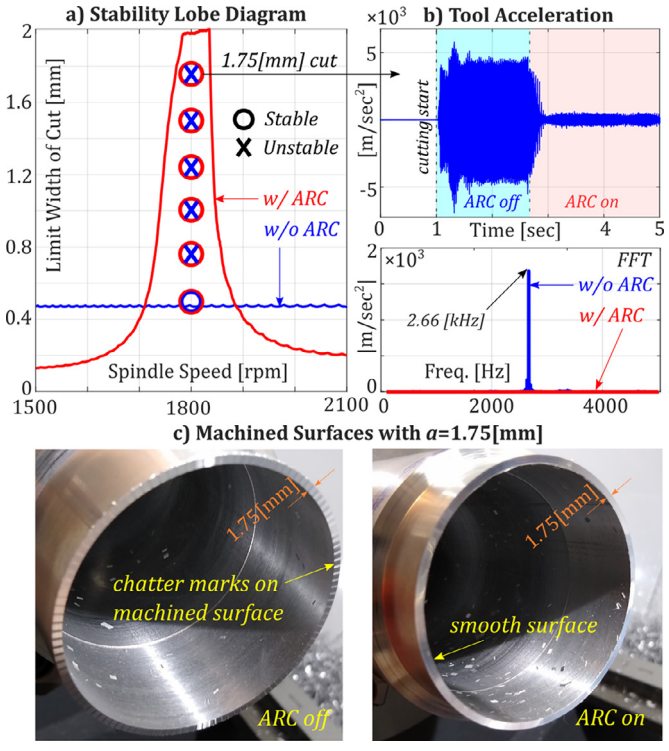

Fig. 6. Experimental cutting results.

Lastly, ARC is implemented to create lobes at different spindle speeds such as at 1000 and 1400[rpm] to showcase its flexibility and robustness to increase MRR on demand in Fig. 7. As shown, ARC can be tuned to create large stability lobes at various speeds. In comparison, delayed feedback control [12] can only provide minor improvement and requires tedious manual gain tuning.

5. Conclusions

The objective of this paper was to design a controller to mitigate high frequency chatter vibrations using machine tool feed drives. An FTS drive

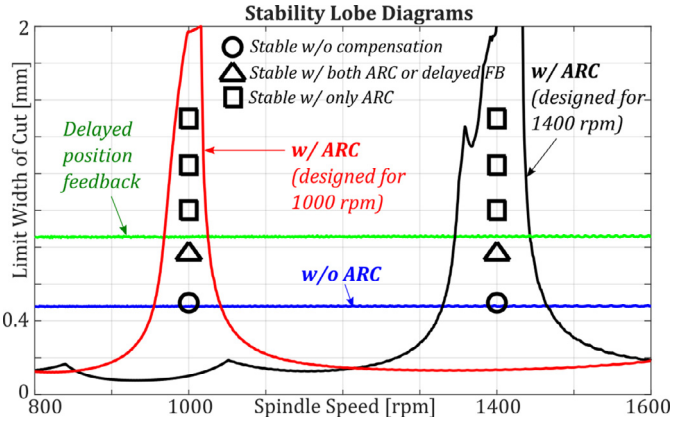

Fig. 7. Chatter stability lobe (SLD) shaping by proposed technique.

with a closed loop positioning bandwidth of <1 kHz is used, and regenerative chatter vibrations occurring at 2.66 kHz are attenuated. Stability lobes are shaped to realize 4 × higher MRR in a desired cutting speed range. Proposed compensator is designed to be used in conjunction with an existing position controller to realize both low frequency tool positioning and high frequency chatter mitigation as long as the feed drive can transmit small motion around the chatter frequency. Therefore, it works best with a FTS, but it can also be implemented on active damper systems such as in inertial actuators [5-10]. Implementation in chatter-experiencing machining processes other than turning requires process kinematics to be embedded in the controller design.

Declaration of Competing Interest

The authors declare that they have no known competing financial interests or personal relationships that could have appeared to influence the work reported in this paper.

Acknowledgment

Authors gratefully thank University of British Columbia (UBC)'s Manufacturing Automation Laboratories (MAL) for assisting with the experimental setup, and NSF (Award No: 1661926) for partially funding this research.

References

[1] Altintas Y, Weck M (2004) Chatter stability in metal cutting and grinding. *Annals of the CIRP* 53(2):619–642.
[2] Munoa J, Beudaert X, Dombovari Z, Altintas Y, Budak E, Brecher C, Gtepan G (2016) Chatter suppression techniques in metal cutting. *Annals of the CIRP* 65(1):785–808.
[3] Budak E, Tunc LT (2010) Identification and modeling of process damping in turning and milling using a new approach. *Annals of the CIRP* 59(1):403–408.
[4] Shamoto E (2012) A novel tool path/posture optimization concept to avoid chatter vibration in machining–proposed concept and its verification in turning. *Annals of the CIRP* 61(1):331–334.
[5] Munoa J, Mancisidor I, Loix N, Uriarte LG, Barcena R, Zatarain M (2013) Chatter suppression in ram type traveling column milling machines using a biaxial inertial actuator. *Annals of the CIRP* 62(1):407–410.
[6] Lu X, Chen F, Altintas Y (2014) Magnetic actuator for active damping of boring bars. *Annals of the CIRP* 63(1):369–372.
[7] Chen F, Hanifzadegan M, Altintas Y, Lu X (2015) Active damping of boring bar vibration with a magnetic actuator. *IEEE ASME Trans Mechatronics* 20(6):2783–2794.
[8] Zaeh MF (2017) Automatic tuning of active vibration control systems using inertial actuators. *Annals of the CIRP* 66(1):365–368.
[9] Abele E, Altintas Y, Brecher C (2010) Machine tool spindle units. *Annals of the CIRP* 59(2):781–802.
[10] Munoa J, Beudaert X, Erkorkmaz K, Iglesias A, Barrios A, Zatarain M (2015) Active suppression of structural chatter vibrations using machine drives and accelerometers. *Annals of the CIRP* 64(1):385–388.
[11] Van Dijk NJM (2012) Robust active chatter control in the high-speed milling process. *IEEE Trans Control Syst Technol* 20(4):901–917.
[12] Mancisidor I (2019) Delayed feedback control for chatter suppression in turning machines. *Mechatronics* 63(1):102276.
[13] Altintas Y, Woronko A (2002) A piezo tool actuator for precision turning of hardened shafts. *Annals of the CIRP* 51(1):303–306.